Earthquake-Induced Rock Fall Hazard Zonation of Varzeghan-Ahar Region in Northwest Iran: A Comparison of Quantitative and Qualitative Approaches

Mohammadreza Mahdavifar[1], Faradjollah Askari[2*], Parham Memarian[3], and Majid Seyedimorad[4]

1. Assistant Professor, Geotechnical Engineering Research Center, International Institute of Earthquake Engineering and Seismology (IIEES), Tehran, Iran
2. Assistant Professor, Geotechnical Engineering Research Center, International Institute of Earthquake Engineering and Seismology (IIEES), Tehran, Iran,
* Corresponding Author; email: askari@iiees.ac.ir
3. Ph.D. Candidate, Geotechnical Engineering Research Center, International Institute of Earthquake Engineering and Seismology (IIEES), Tehran, Iran
4. M.Sc. Graduate, College of Science, University of Tehran, Tehran, Iran

Received: 17/10/2015
Accepted: 14/06/2016

ABSTRACT

In this study, three earthquake-induced rock fall hazard maps of the regions affected by Varzeghan-Ahar earthquake doublet are presented. On August 11, 2012 an earthquake doublet (Mw= 6.5 and, Mw= 6.3) struck Varzeghan, Ahar and Heris regions (located in Azerbaijan-e-Sharghi province of Iran). Most of the landslides triggered by the earthquakes were rock falls and disrupted rock slides. Several rock fall zones, some with more than 150 rock falls were recorded, the farthest one approximately 45 kilometers away from the earthquake epicenters. A landslide inventory map of the region was prepared using field survey gathered data and satellite imagery analysis. Three methods of Information Value (IV), Logistic Regression (LR), and Analytical Hierarchy Process (AHP) were used for earthquake-induced rock fall hazard zonation. LR and IV are quantitative landslide hazard zonation methods, and AHP is a qualitative one. The results from each method were then compared using Receiver Operating Characteristics (ROC) curve. The area under ROC curve (AUC) was 0.927, 0.90, and 0.898 for LR, IV, and, AHP models, respectively. LR seems to be the most suitable method for the study, although all three methods have approximately similar qualities.

Keywords:
Landslide hazard zonation; Rock fall; Earthquake-induced landslides; Varzeghan-Ahar earthquake; Logistic Regression; Information Value; Analytical Hierarchy Process

1. Introduction

Earthquake-induced landslides have an immense impact on fatality and financial loss increase during earthquakes. In many earthquakes, the triggered landslides have caused as much damage as ground seismic shaking direct effects [1]. Susceptibility and hazard mapping of earthquake-induced landslides can help in disaster mitigation and management as well as urban and regional planning.

On August 11, 2012, two earthquakes with magnitudes of Mw=6.5 and Mw=6.3 struck Varzeghan and Ahar regions in northwest of Iran at 16:53 and 17:04 local time, respectively. Earthquake epicenters were 19 kilometers southeast of the town of Varzeghan with focal depth of about nine and four kilometers, respectively. The earthquakes had strike-slip and reverse mechanisms [2]. The

maximum peak ground acceleration was recorded by Varzeghan station of about 532 cm/s/s from the second event [3]. These events resulted in 258 fatalities and about 1380 injuries and caused severe damages to the villages and cities in the region [4]. Most fatalities and injuries were reported from Bajebaj, Gouradareh and Damanabad villages and Varzeghan town. Maximum intensity of the earthquake in the scale of EMS98 was VIII+ at epicenter zone; and VII, VI and V for Ahar, Heris and Tabriz cities, respectively (Figure 1). Many landslides were triggered by the earthquakes mostly of rock fall and rock slide types [5].

Conventionally, in landslide hazard zonation studies a single map is presented for all different landslide types and landslide triggering factors, while considering the type of any single landslide or triggering factor can widely improve the resultant hazard map [6-7]. Rock falls and disrupted rock slides are the most abundant landslides triggered by earthquakes, which cause direct and indirect damages such as: fatalities, infrastructures destruction, and roads blockage [8-9]. In this study, earthquake-induced rock fall hazard of Varzeghan-Ahar area is investigated.

Various methods utilized for landslide hazard analysis by different researchers can be categorized into two main approaches: qualitative, and quantitative. Qualitative methods are mainly based on expert judgment and depend on pre-knowledge and experience of the expert. In this sense, they are more subjective. Quantitative methods, on the other hand, are based on direct numerical analysis of gathered data for landslide hazard estimation and so are rather objective [10-15].

Landslide hazard estimation methods can also be divided into three main types of deterministic, statistical, and heuristic. Deterministic and statistical methods are quantitative. Using geotechnical, topographical and groundwater data, deterministic methods are the most precise of all three to analyze stability of slopes and are used for large scale studies. Statistical methods are mainly based on data analysis of past landslides to determine future ones. Statistical approaches are divided to two types of bivariate and multivariate. In bivariate statistical method, any causative factor is analyzed individually. Inversely, in multivariate method, all causative

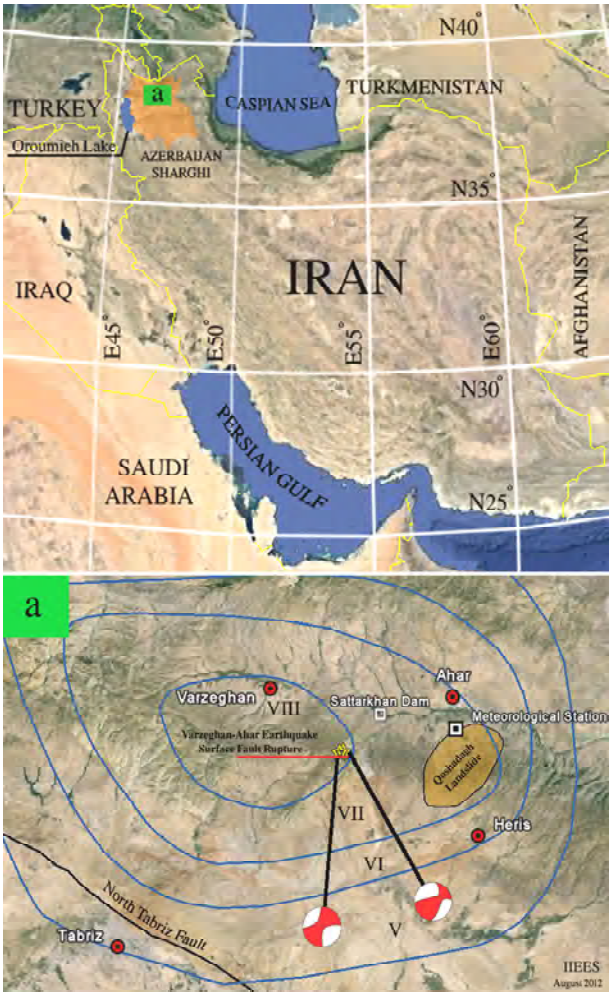

Figure 1. Index map and iso-intensity map of Varzeghan-Ahar earthquake doublet [19].

factors are taken into account simultaneously and so relative contribution of the factors is determined. Heuristic methods are mostly qualitative, in which factors are weighted based on their assumed importance in landslide occurrence, and then the landslide hazard map is produced combining the causative factor weights [16-18].

Earthquake-induced rock fall hazard maps for Varzeghan-Ahar region are prepared and compared using two quantitative and one qualitative method. The two quantitative methods are Information Value (IV) and Logistic Regression (LR), which are bivariate and multivariate statistical, respectively; and analytical Hierarchy Process (AHP) is the semi-qualitative heuristic one.

2. Regional Settings

2.1. Tectonics and Seismicity

Northwest of Iran tectonics is affected by the

movement of Arabian plate toward Eurasian plate. The total movement rate is 22 mm/year [20]. This movement at the longitude of northwest of Iran and eastern Turkey is in a northwest direction [21]. WNW-ESE Right lateral Strike-slip faulting in the region is in agreement with this movement (e.g. North Tabriz Fault with 7 mm/year rate [22]). The shortening component of the movement mostly results in thrust faulting in the northern area of Caucasus [23]. The Varzeghan-Ahar earthquake locates in the zone of right-lateral strike-slip faulting within Turkish-Iranian Plateau. Varzeghan-Ahar causative fault was an active but unrecognized fault in the north of famous North Tabriz Fault. The surface fault rupture length has been measured about 13 km on field investigations and is proved to be related to first event [21].

Northwest of Iran is a highly seismic area with several huge historical earthquakes. Seven historical earthquakes have occurred with estimated magnitudes ranging from 6 to 7.7 within the study area [24-25]. Furthermore, ten instrumental earthquakes with magnitudes greater than 4 have been recorded in the study area (Figure 2) [26]. The nearest historical earthquake has occurred on 1856 about 35 kilometers southwest of the Varzeghan-Ahar earthquake epicenters and the nearest instrumental earthquake before Varzeghan-Ahar earthquake has a magnitude of 4 and is 10 kilometers far from the Varzeghan-Ahar earthquake epicenters [24, 26]. Nevertheless, Varzeghan-Ahar earthquake doublet (1st event: Mw = 6.5, Focal Depth=9 km; 2nd

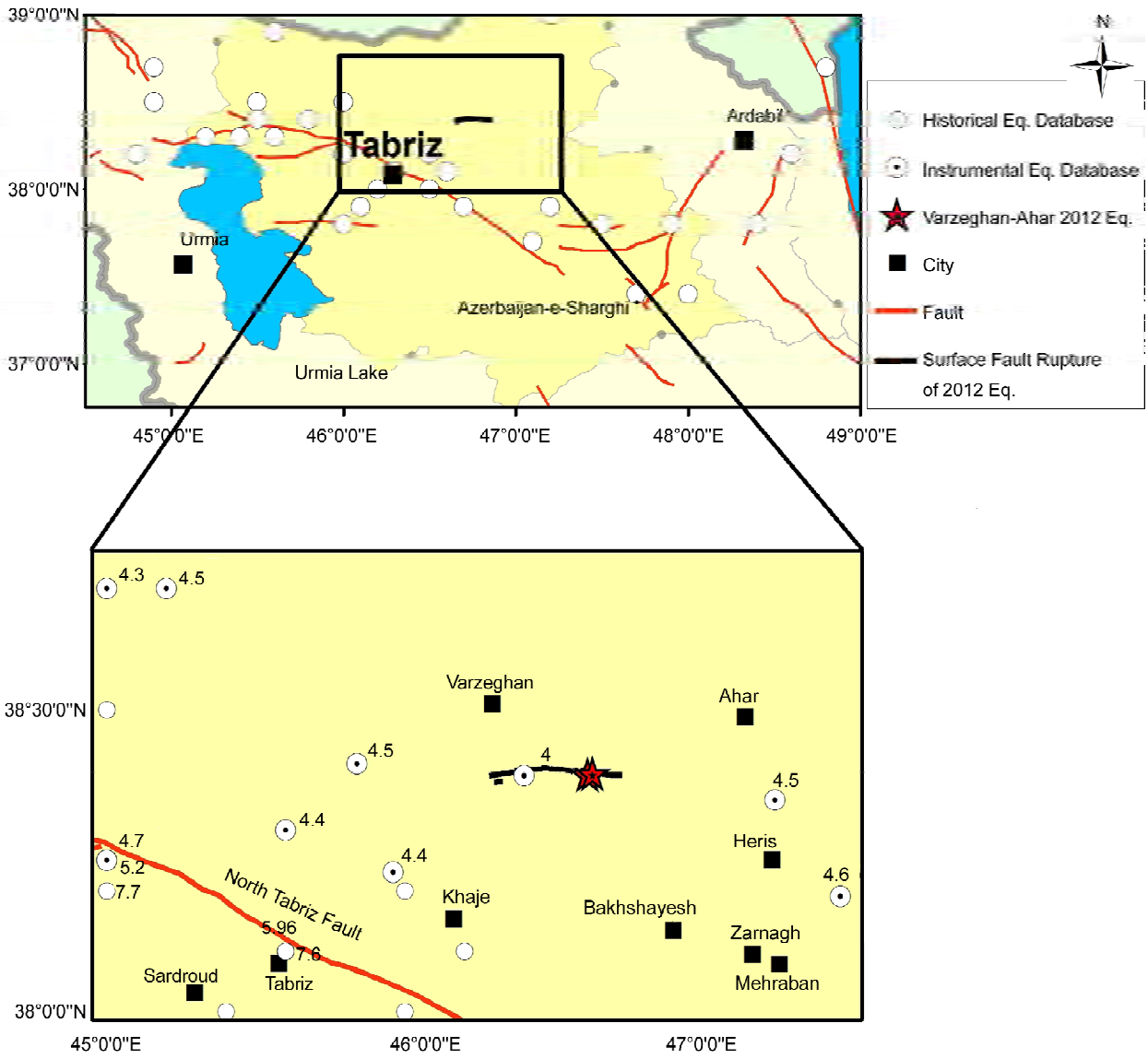

Figure 2. Historical and Instrumental earthquakes epicenters in the study area (numbers are Mw magnitudes) [24, 26].

event: Mw = 6.3, Focal depth = 4 km) is still the largest event of its causative fault in the entire earthquake catalogue. Having numerous aftershocks this earthquake reduced a big part of accommodated stress in the region [27].

2.2. Climate

Varzeghan-Ahar region has a continental Mediterranean climate, characterized by seasonality in temperature. A Mediterranean climate is defined as having mild and rainy winters and long, hot and dry summers [28]. However, the Mediterranean climate in northwest of Iran has cold and snowy winters [28-29]. The precipitation of the region is affected by Mediterranean wet air masses, Siberian cold northern weather effects, and temperature variations near Urmia Lake [30].

Based on Ahar meteorological station data (23 kilometers east of the earthquake epicenters), mean annual precipitation of the region ranges from 205 to 340 mm. Annual precipitation from August 1st 2011 was 338.4 mm, and the last rainfall of 4 mm occurred on August 1st 2012, 10 days before the earthquake. Total precipitation from May 1st to August 11th, when the earthquake occurred, was 109.6 mm [31].

2.3. Geology

Varzeghan-Ahar area is underlain by a wide variety of sedimentary and volcanic rocks and unconsolidated sedimentary deposits, most of which belong to the period from Cretaceous through Quaternary. The rocks vary greatly in composition, degree of consolidation and depth of weathering. Marl, Sandstone and Volcanic rocks predominate. Based on 1:250,000 geologic maps of Ahar and Tabriz-Poldasht [32, 33] and considering geologic time era and predominant material type, geology map of the area can be categorized as:

1. Creataceous Extrusive Igneous Rocks (Cr1);
2. Creataceous Limestone and Conglomerate Rocks (Cr2);
3. Creataceous Marly Rocks (Cr3);
4. Paleogene Igneous Rocks (PG1);
5. Paleogene Marly Rocks (PG2);
6. Paleogene Conglomerate Rocks (PG3);
7. Neogene Extrusive Igneous Rocks (NG1);
8. Neogene Pyroclastic Rocks (NG2);
9. Neogene Marly Rocks (NG3);
10. Neogene Conglomerate Rocks (NG4);
11. Quaternary Alluviums (Q1);
12. Quaternary Igneous Rocks (Q2);

Figure (3) depicts the geological classification of the study area.

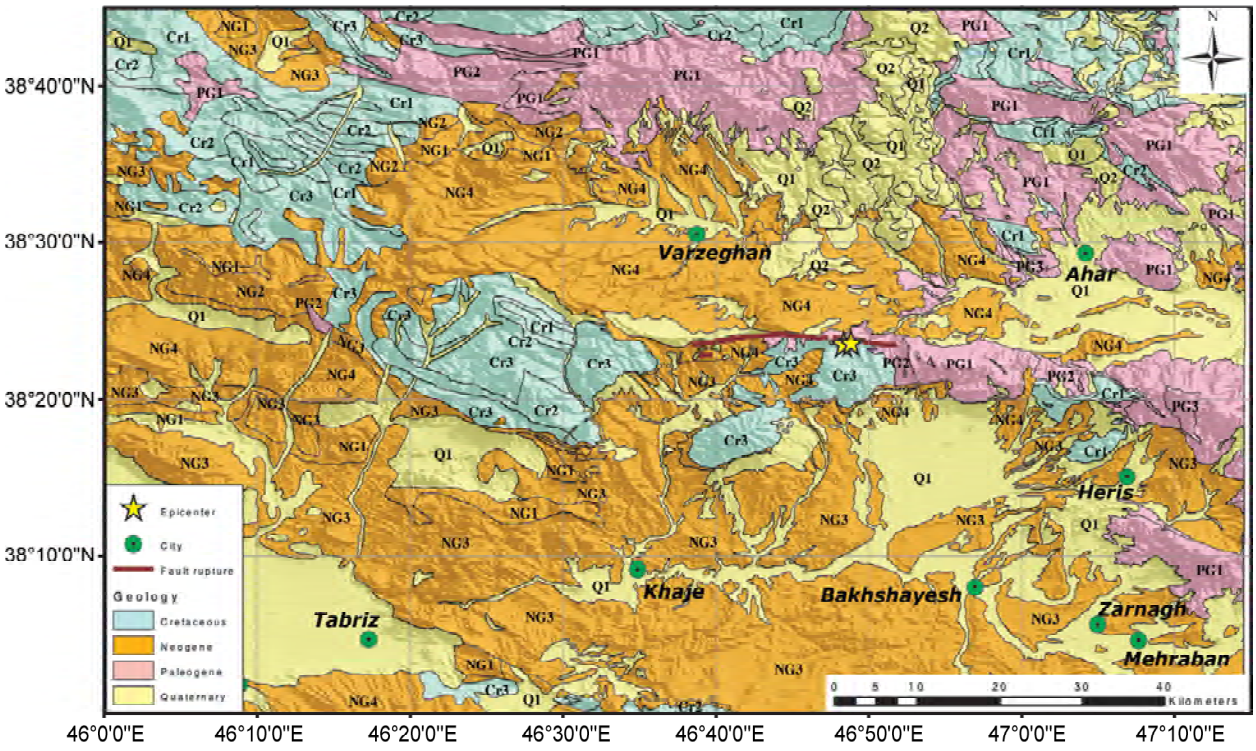

Figure 3. Geology map of the study area [32-33].

3. Coseismic Landslide Inventory of Varzeghan-Ahar Earthquake

The region has a high potential of landsliding, due to landslide-sensitive lithology and mountainous topography; there are a lot of old landslides all over the area. Additionally, north part of Iran including the study area is exposed to the effects of the less frequent but more energetic earthquakes, which is the prerequisite of huge earthquake-induced landslides [34]. Twenty kilometers east of Varzeghan-Ahar earthquake epicenters locates Qoshadagh gigantic prehistoric earthquake-induced landslide. Qoshadagh prehistoric landslide with an estimated volume of 83-110 cubic kilometers is one of the most voluminous subaerial gravitational slope failures known on earth [35].

A field survey was organized 17 days after the earthquake to determine earthquake-induced landslides distribution and characteristics. Data gathered by two other groups from International Institute of Earthquake Engineering and Seismology (IIEES) and a group from Geological Survey of Iran (GSI) were also considered.

Fourteen coherent landslides, hundreds of disrupted landslides, several lateral spreads and one soil flow were recorded [5].

Varzeghan-Ahar earthquake triggered eight soil block slides, three soil slumps, two rock block slides, and one rock slump, which are classified as coherent landslides [9]. Coherent landslide inventory of Varzeghan-Ahar earthquake doublet is shown in Table (1) and some of them are shown in Figures (4) to (6).

Number of disrupted rock slides and falls for parts of the region, visited on the field survey, were determined from direct count. Totally 28 rock fall zones with 491 rock falls were recorded during site visit, entitled as "recorded inventory". The farthest recorded rock fall zone with 50 kilometers distance from earthquake epicenters and the rock fall trajectory is shown in Figures (7) to (9).

Based on recorded rock fall inventory properties and densities, an artificial rock fall inventory of the study area was produced. Firstly, the recorded rock

Figure 4. Soil block slide near Karavigh village (Photo by M.R. Mahdavifar, August 31st 2012).

Figure 5. Bajebaj rock block slide scarp (Photo by M.R. Mahdavifar, August 30th 2012).

Figure 6. Biggest Nasirabad reactivated soil slump (Photo by M.R. Mahdavifar, August 30th 2012).

Table 1. Varzeghan-Ahar earthquake-induced coherent landslides properties.

Landslide No.	Distance to Fault Rupture	Distance to Epicenter	Type[a]	Formation Group	Slope Condition	Length[b]	Width[c]	Reactivated landslide
1	500 m	4.0 km	Rock Slump	NG4	-	25 m	75 m	No
2	200 m	3.5 km	Soil Slump	NG4	Grassy Hill	20 m	70 m	No
3	5.1 km	12.9 km	Soil Slump	Q1	Next to Swamp - Road Is Destroyed	25 m	50 m	No
4	5.2 km	7.0 km	Soli Block Slide	NG4	Next to Spring	22 m	15 m	No
5	2.4 km	4.2 km	Soil Slump	Cr3	Grassy Hill	16 m	39 m	No
6	8.5 km	11 km	Rock Block Slide	Q1	Next to Road-Road is Blocked	6 m	25 m	No
7	16.5 km	20.0 km	Soil Block Slide	NG4	Next to River	5 m	40 m	No
8	4.2 km	6.7 km	Rock Block Slide	Cr3	Bajebaj Rock Block Slide	95 m	65 m	Yes
9	1.4 km	5.5 km	Soil Slump	NG4	Grassy Hill	28 m	48 m	Yes
10	9.6 km	12.4 km	Soil Slump	Q1	Landsliding Zone of Nasirabad Village	30 m	90 m	Yes
11	8.9 km	11.6 km	Soil Slump	Q1	Landsliding Zone of Nasirabad Village	25 m	60 m	Yes
12	9.5 km	12.2 km	Soil Slump	Q1	Landsliding Zone of Nasirabad Village	90 m	175 m	Yes
13	200m	4.1 km	Soil Slump	NG4	Grassy Hill	30 m	100 m	Yes
14	9.8 km	12.6 km	Soil Slump	Q1	Landsliding Zone of Nasirabad Village	85 m	375 m	Yes

a. For landslide types detailed description refer to Keefer [9]
b. Horizontal distance from top of headscarp to toe (upslope to downslope) [36]
c. Generally the widest dimension across the slope [36]
d. Landslides No. 7, 8, and 14 are shown in Figures (4) to (6), respectively

Figure 7. Rock fall susceptible Neogene formation composed of Marl and Sandstone (Photo by M.R. Mahdavifar, August 29th 2012).

Figure 9. Scratches resulted from falling rocks (Photo by M.R. Mahdavifar, August 29th 2012).

Figure 8. Rock fall trajectory from the crest to the valley (Photo by M.R. Mahdavifar, August 29th 2012).

fall areas properties such as slope angle, geology, earthquake intensity, etc. were derived from prepared thematic maps, and rock fall density of each rock fall zone was calculated. Besides, geomorphologic and surface condition of these areas was investigated using Google earth satellite imagery and aerial photographs. Then, the effective thematic layers (prepared in ARC GIS program), were overlaid on Google earth satellite imagery and the study area was investigated by meticulously considering geomorphologic and surface conditions to find rock fall prone areas. Finally, rock fall zones for artificial inventory were estimated based on recorded inventory properties and expert judgment. The resulting

artificial inventory contains about 420 rock fall zones and 8000 rock falls. Disrupted landslides of recorded and artificial inventories of Varzeghan-Ahar earthquake are shown in Figure (10).

4. Methodology

4.1. Input Layers and Analysis Methods

There are many conditioning and triggering factors used in the literature for landslide hazard zonation. The most important triggering factors are earthquake and rainfall, and most important conditioning factors are slope angle and terrain strength [6, 37]. Furthermore, the importance of affecting factors changes for different landslide types. For example, soil moisture is not an important factor in rock fall occurrence while it is one of the most important factors in soil slump occurrence. In this study, earthquake-induced rock fall hazard zonation is investigated and hence important factors for rock fall occurrence are chosen for analysis. Topographic factors of slope angle, terrain roughness, distance to roads and rivers, slope height, and slope aspect besides geology map and earthquake intensity map are used. Topographic layers are derived from topographical maps of National Cartographic Center of Iran (NCC). Geological data is derived digitizing geologic maps of Ahar and Tabriz-Poldasht [32-33], and earthquake intensity layer is created using published earthquake intensity map of Varzeghan-Ahar earthquake doublet [19].

Three methods of information value, logistic regression and analytical hierarchy process (AHP) are used for earthquake-induced rock fall hazard zonation in Varzeghan-Ahar area. For all of the methods, the input and output datasets are 50 meters cell size maps. The determination of cell size is based on the minimum precision of all causative factors to guarantee the quality of output maps and avoid misleading results.

A dataset with 65 rock fall zones and 1100 rock falls was randomly selected from artificial rock fall inventory to develop models. The models verification is conducted using recorded inventory map. The same input variables of slope angle, geology, earthquake intensity, terrain roughness, distance to roads and rivers, slope height, and slope aspect are used for all methods. To assess the results and compare the accuracy of these three methods, Receiver Operating Characteristics (ROC) curve is used.

4.2. Information Value

Information value is a bivariate statistical method for landslide hazard zonation. In bivariate methods, each independent variable effect on the dependent variable is estimated individually without taking other factors into account. This method wa introduced by Yin and Yan in 1988, and was modified by other researchers as Eq. (1) shown below: [38-39]:

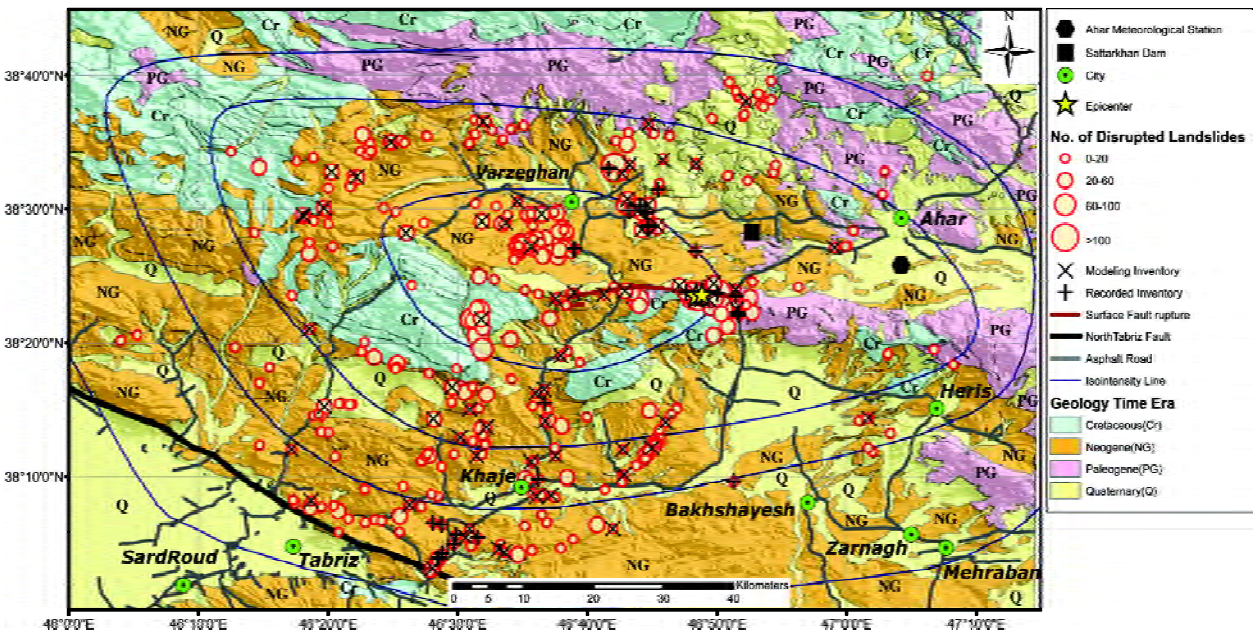

Figure 10. Disrupted rock slides and rock falls distribution.

$$IV = Ln(\frac{p(B/Ai)}{p(B)}) \quad (1)$$

where IV is Information value, $p(B/Ai)$ is the probability of landslide occurrence in Ai class, $p(B)$ is the overall probability of landslide occurrence in the region.

For the sake of simplification, the probability can be substituted by landslide density in the formula. Landslide density for each causative factor classes is calculated using landslide artificial inventory of the study area. In some researches, the area of landslides (land unit areas or area of pixels occupied by landslides) is used for density calculation, and in some others the number of landslides are used for calculations [40-41]. In this research, the following formula (Eq. 2) is used for information value calculation [39, 41].

$$IV = Ln(\frac{Ni/Ai}{Nt/At}) \quad (2)$$

where IV is information value, Ni is number of landslides in class i, Ai is the area of class i, Nt is total number of landslides, and At is total area of the study area.

Causative factors contributing in landslide occurrence are categorized to different classes and the IV weight of each class is calculated as shown in Table (2). Because of the logit format of the formula, for classes with no landslide, it results in undefined values, to solve this problem a single landslide is assumed for such classes [42]. Finally,

Table 2. Information Value and AHP weights for different causative factor classes.

Factor	Class Description	No. of Rock Falls in Class	Area of the Class (Pixels)	Information Value (IV)	AHP Weight
Slope Angle (Degree)	0-5	74	1346364	-1.71	0.009
	5-10	33	729208	-1.91	0.014
	10-15	171	510385	0.09	0.03
	20-30	201	379625	0.55	0.046
	15-20	246	477109	0.52	0.062
	>30	371	148692	2.10	0.11
Geology	Cr1	1	211669	-4.17	0.01
	Cr2	1	141512	-3.77	0.012
	Cr3	150	215074	0.82	0.048
	PG1	1	395222	-4.80	0.006
	PG2	52	63787	0.98	0.049
	PG3	1	7036	-0.77	0.031
	NG2	94	91672	1.21	0.046
	NG3	1	63082	-2.96	0.018
	NG4	184	835333	-0.33	0.035
	NG5	347	507634	0.80	0.042
	Q1	269	946519	-0.08	0.036
	Q2	1	112843	-3.54	0.014
Earthquake Intensity	IV	1	276416	-4.44	0.006
	V	85	1203113	-1.46	0.015
	VI	118	873397	-0.82	0.022
	VII	491	952054	0.52	0.049
	VIII	402	286403	1.53	0.075
Terrain Roughness	Convex	679	1660559	0.29	0.021
	Flat	19	362747	-1.76	0.006
	Concave	398	1568077	-0.18	0.012
Disturbance Distance (m)	0-200	347	448907	0.93	0.032
	200-700	285	870784	0.07	0.022
	700-2200	341	1508762	-0.30	0.012
	>2200	123	762930	-0.64	0.007
Slope Height (m)	0-15	556	2576550	-0.35	0.003
	15-60	495	896416	0.59	0.005
	60-500	45	116582	0.23	0.01
	>500	1	1835	-1.72	0.001
Aspect	Flat	6	250645	-2.55	0.006
	N	90	382809	-0.26	0.011
	NE	36	371423	-1.15	0.007
	E	93	382219	-0.23	0.009
	SE	185	440859	0.32	0.011
	S	132	441758	-0.02	0.012
	SW	127	477272	-0.14	0.008
	W	160	425981	0.21	0.014
	NW	267	418417	0.74	0.013

the summation of weights derived by analyzing all thematic map categories is calculated. The higher the total value of IV, the higher the susceptibility to landsliding is. Zero value represents landslide probability equal to mean landslide probability of the whole region.

4.3. Logistic Regression

Binomial or Binary logistic regression is a multivariate statistical method introduced by cox 1958 [43]. When the dependent variable is a dichotomy, binary logistic regression is a good choice for statistical analysis.

In multivariate methods the relationship between any of independent variables and dependent variable is estimated simultaneously with all other causing factors.

Comparing with linear regression method it has two important benefits, firstly in opposite to linear regression variables do not need to have normal distribution. Secondly, independent variables may be either continuous or categorical, or any combination of these two [44].

In binary logistic regression model, the independent variables (causative factors) coefficients are estimated by the maximum likelihood method. Logistic regression formulation has the form of Eq. (3).

$$Logit(y) = \beta_0 + \beta_1 X_1 + \beta_2 X_2 + ... + \beta_i X_i + e \quad (3)$$

where, y is the dependent variable, X_i is the i^{th} independent variable, β_0 is a constant, X_1 is the i^{th} regression coefficient and e is the error. The probability (p) of variable "y" occurrence is calculated as Eq. (4).

$$P = \frac{\exp(\beta_0 + \beta_1 X_1 + \beta_2 X_2 + ... + \beta_i X_i)}{1 + \exp(\beta_0 + \beta_1 X_1 + \beta_2 X_2 + ... + \beta_i X_i)} \quad (4)$$

The resulting relationship describes how landslide occurrence is related to different causative factors. The dependent input variable of logistic regression method should have binary form where 1 represents landslide presence and 0 means no landslide occurrence in a specific area.

Besides, 1100 rock falls selected from artificial inventory, 1100 points with no rock fall were chosen randomly to develop LR model.

Wald test is used to assess significance of the coefficients given by LR model. It is calculated by comparing maximum likelihood estimate of each coefficient with the estimated standard error of it as shown in Equation 5. The dependent variable's coefficient sign reveals its effect on probability of landslide occurrence [45]. LR method resulted coefficients and Wald values are shown in Table (3).

Table 3. Logistic Regression coefficient for different causative factor.

Factor	β[a]	SE[b]	Wald[c]
Slope Angle	0.1145	0.007	288.47
Geology	0.2382	0.02	140.79
Earthquake Intensity	0.7817	0.065	143.53
Slope Height	0.0023	0.002	1.06
Terrain Roughness	-0.1091	0.102	1.14
Disturbance Distance	-0.0009	0.00008	127.45
Aspect	0.0028	0.001	19.49
Constant	-10.129	0.534	360.29

a. Factor Coefficient b. Standard Error c. Wald test Value

$$Wald = \left(\frac{\beta}{SE} \right)^2 \quad (5)$$

Considering Wald values given in Table (3), slope angle, earthquake intensity, and geology are the most effective factors in rock fall occurrence, respectively. The positive sign of the coefficients infers that they are directly related to rock fall occurrence probability, and the negative sign shows inverse relation.

4.4. Analytical Hierarchy Process

Analytical hierarchy process (AHP) is a decision-making method based on pairwise relative comparison of contributing factors. Priority scales are determined by expert judgment [46-48]. The comparison aims to define how much a factor dominates another in forming a result, and in this way mathematizes the decision-making process.

AHP method has following four main steps [47, 49, 50]:

1. Define the problem and break it down to the contributing factors and their components.
2. Arrange the structure of the model in a hierarchical order with the goal of the model at top, proceeding with the contributing factors, and the subdivisions of the contributing factors.
3. Perform a pairwise comparison between model elements and construct a set of pairwise

Table 4. Scale of preference between two elements in AHP [47].

Intensity of Importance	Definition	Explanation
1	Equal Importance	Two activities contribute equally to the objective
2	Weak or slight	
3	Moderate importance	Experience and judgment slightly favor one activity over another
4	Moderate plus	
5	Strong importance	Experience and judgment strongly favor one activity over another
6	Strong plus	
7	Very strong or demonstrated importance	An activity is favored very strongly over another; its dominance demonstrated in practice
8	Very, very strong	
9	Extreme importance	The evidence favoring one activity over another is of the highest possible order of affirmation
Reciprocals of above	If activity i has one of the above non-zero numbers assigned to it when compared with activity j, then j has the reciprocal value when compared with i	A reasonable assumption
1.1–1.9	If the activities are very close	May be difficult to assign the best value but when compared with other contrasting activities the size of the small numbers would not be too noticeable, yet they can still indicate the relative importance of the activities.

comparison matrices including priority scales.

4. Analyze the resulted matrices and determine weight of contribution of each element.

The priority of each element to another is determined by the scores given in Table (4).

The judgments may be inconsistent. A concern of the AHP is how to measure inconsistency and improve the judgments when possible in order to obtain better consistency [47].

The AHP model results consist of AHP weights and Consistency Ratio (CR). Consistency ratio is calculated as shown in Eq. (6). It specifies the probability that assumed weights are randomly selected.

$$CR = \frac{CI}{RI} \tag{6}$$

where, CR is Consistency Ratio, RI is the average of the resulting consistency index and, CI is con-sistency index calculated as Eq. (7):

$$CI = \frac{(\lambda_{\max} - n)}{(n-1)} \tag{7}$$

where CI is consistency index, $\lambda_{\max}$ is the largest or principle eigenvalue of matrix and, n is the order of the matrix. Consistency ratios less than 0.1 are usually accepted, but for values greater than 0.1 the weights may need to be revised [51].

A pairwise comparison for contributing factors and then for their classes was conducted. Table (5) shows the pairwise comparison of main contributing factors, assumed priority scales, and resulting weights. For brevity, only the final weights for classes of contributing factors are shown in Table (2). As shown in Table (2), the overall inconsistency is CR = 0.02, which locates in the accepted domain.

Table 5. Main contributing factors priority scales and resulted weights.

Factors	Slope Angle	Earthquake Intensity	Geology	Disturbance Distance	Terrain Roughness	Aspect	Slope Height	AHP Weight
Slope Angle	1	2	3	4	5	6	7	0.354
Earthquake Intensity	1/2	1	2	3	4	5	6	0.240
Geology	1/3	1/2	1	2	3	4	5	0.159
Disturbance Distance	1/4	1/3	1/2	1	2	3	4	0.104
Terrain Roughness	1/5	1/4	1/3	1/2	1	2	3	0.068
Aspect	1/6	1/5	1/4	1/3	1/2	1	2	0.045
Slope Height	1/7	1/6	1/5	1/4	1/3	1/2	1	0.031
CR=0.02								

5. Discussion and Results

The precision of the artificial expert-estimated rock fall inventory used for rock fall hazard zonation, was evaluated by comparing it with earlier researches [9, 52-55]. The maximum area affected by rock fall based on artificial inventory was about 4500 square kilometers, total number of estimated rock falls was about 8000, and the farthest rock fall zone was approximately 45 kilometers away from the earthquake epicenters. Affected area by Varzeghan-Ahar earthquake-induced disrupted landslides and the farthest one to epicenter is shown in Figure (11) in comparison with earlier studies. Based on Keefer 1984 [9], 1000 to 10000 rock falls are expected from such an earthquake. Predicted number of rock falls for the study area is near the uppermost boundary of Keefer [9]. One reason is the doublet nature and relatively numerous after-shocks of the earthquakes [27]. First earthquake triggers a number of rock falls and then the second earthquake with nearly the same magnitude triggers more rock falls on slopes weakened but probably not moved by the first one. This phenomenon is demonstrated by Parker (2015)[56], and is widely seen in landslides with brittle type failure, such as rock falls.

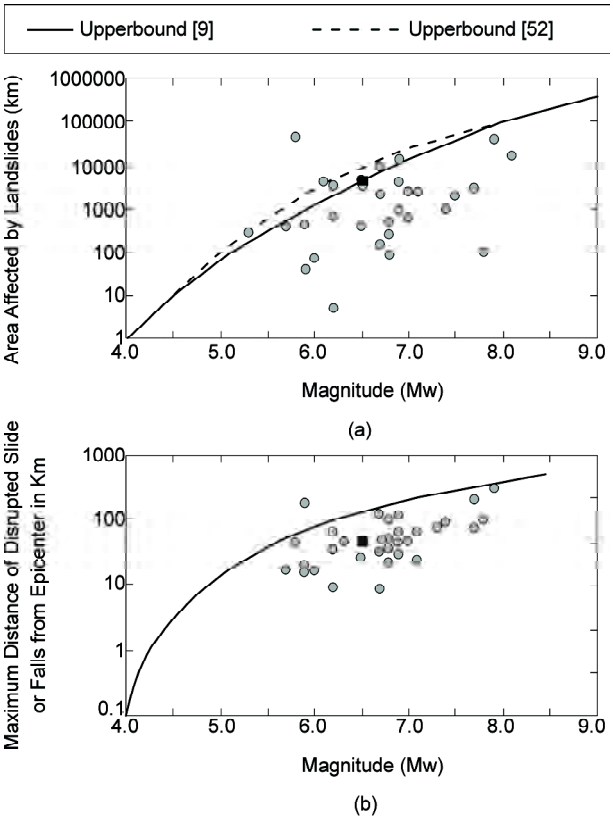

Figure 11. a) Area affected by disrupted landslides. b) Maximum distance of disrupted landslide from epicenter. Dark square represents Varzeghan-Ahar earthquake, and gray circles represent historic earthquakes from earlier studies [52-55].

A sensitivity analysis was conducted to determine appropriate input parameters to preserve in the landslide hazard estimation models. For this purpose, four new IV models were prepared excluding the second-class parameters of Terrain Roughness, Slope Aspect, Disturbance Distance, and Slope Height. Comparing these four models with main IV model results, a reduction in accuracy was observed. Accordingly, all aforementioned parameters, besides Slope Angle, Earthquake Intensity, and Geology were used to create models.

The resulting landslide hazard maps of the region are presented in Figures (12) to (14) for *IV*, *LR*, and *AHP* methods, respectively. Hazard maps are classified into five classes of Very low, Low, Medium, High, and Very high. To assess the classification appropriateness, Relative landslide density (R-index) is used defined as Eq. (8) [57]. Rock fall recorded inventory is used for R-index calculation.

$$R = \frac{Ni / Ai}{Nt / At} \times 100 \tag{8}$$

where R is Relative landslide density, Ni is number of landslides in hazard class i, Ai is the area of hazard class i, Nt is total number of landslides, and At is total area of the study area.

R-index values are presented in Table (6). Landslide densities increase rapidly for very low to very high hazard classes, which demonstrate good quality of classification.

To evaluate and compare the models, receiver operating characteristic (ROC) curve was used with rock fall recorded inventory as verification data [58-59]. ROC curve is the plotted True Positive Ratio (TPR) versus False Positive Ratio (FPR). In current study, TPR or sensitivity is the probability

Table 6. R-index values for hazard maps.

Hazard Class	LR	IV	AHP
Very low	0.03	0.23	0.27
Low	0.66	1.73	1.65
Medium	2.36	3.89	3.22
High	18.06	14.76	12.61
Very high	78.89	79.38	82.26

that a rock fall cell is correctly distinguished by the model, and TNR (True Negative Ratio) or specificity is the probability that a non-rock fall cell is correctly distinguished by the model. FPR is described as 1-specificity (TNR). The diagonal line in ROC curve represents randomly selected data and is called the line of no-discrimination. The area under the ROC curve, known as AUC, represents the accuracy of the model for predicting the landslide hazard. ROC curve from the three methods and resulting AUC values are presented in Figure (15) and Table (7), respectively.

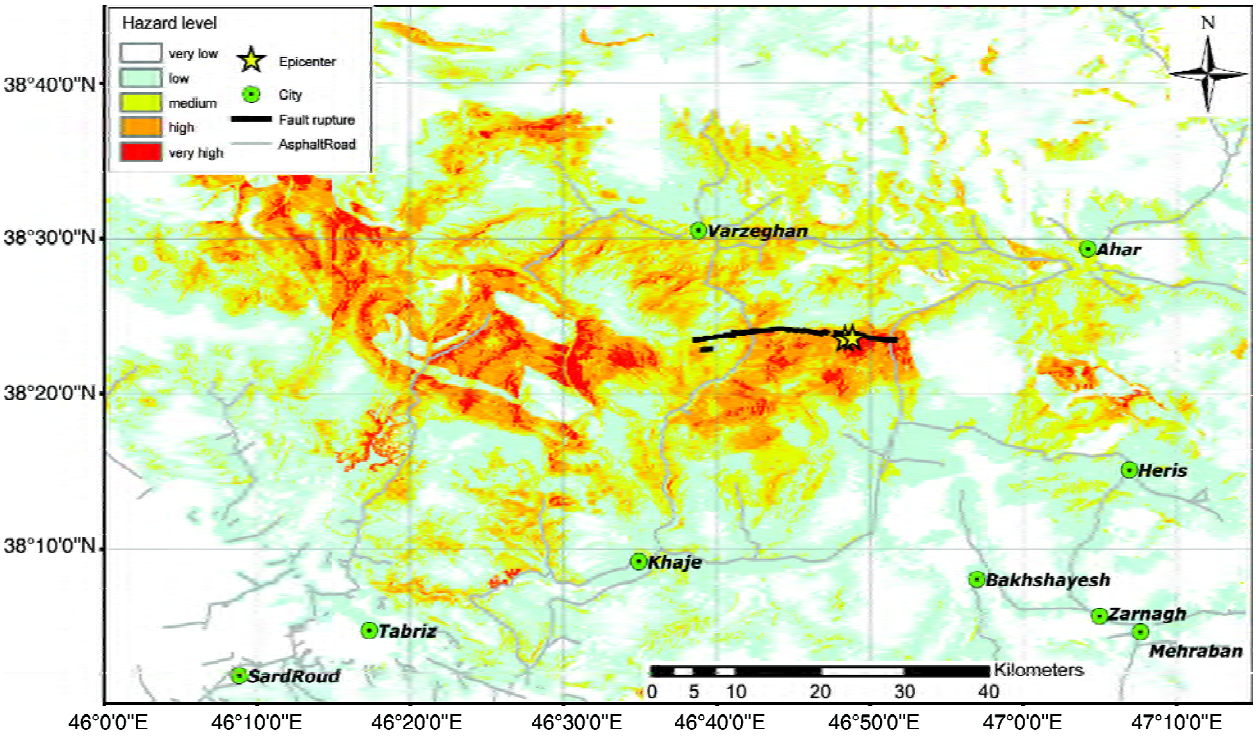

Figure 12. IV method landslide hazard zonation map.

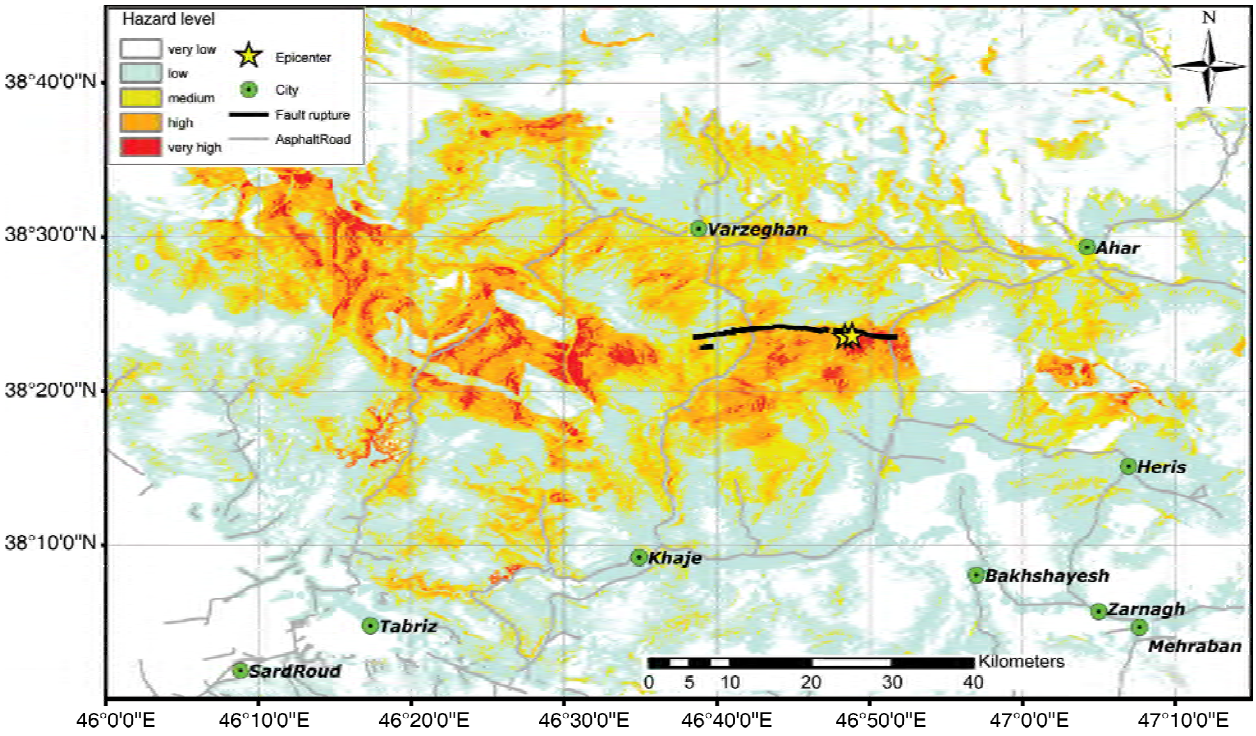

Figure 13. LR method landslide hazard zonation map.

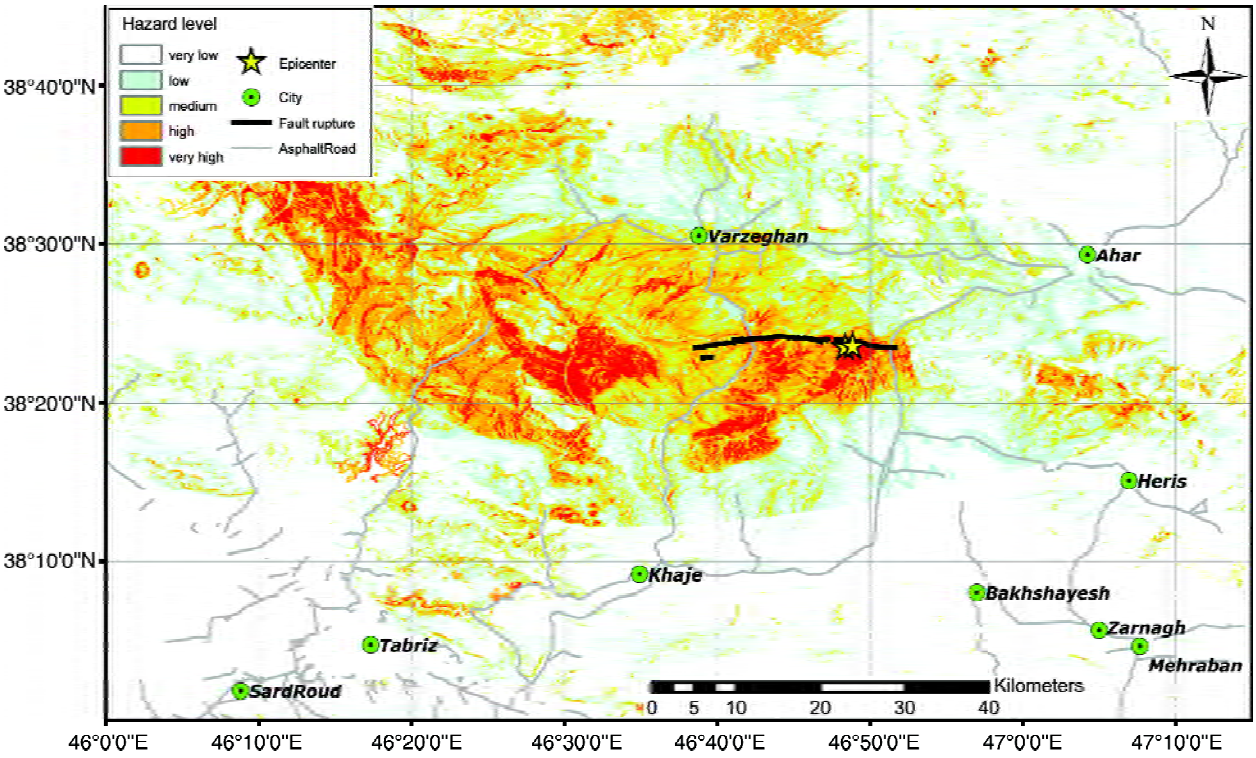

Figure 14. AHP method landslide hazard zonation map.

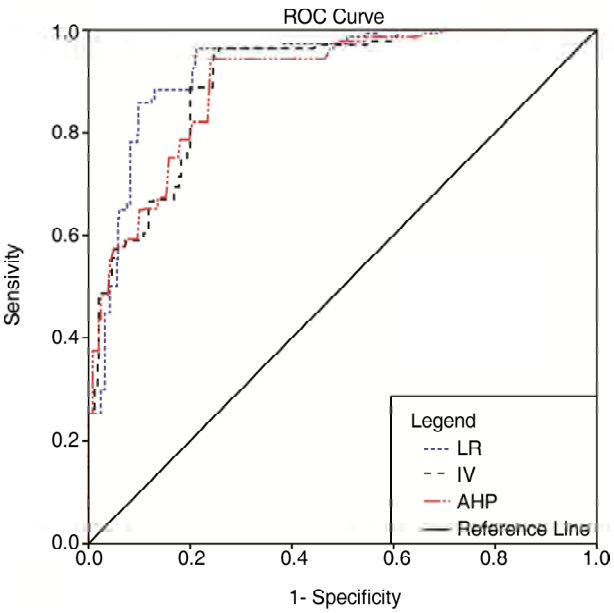

Figure 15. ROC curve for three methods of IV, LR, and AHP.

Table 7. ROC curve properties for three methods.

Test Result Variable (s)	AUC	Std. Error	Asymptotic 95% Confidence Interval	
			Lower Bound	Upper Bound
LR	0.927	0.008	0.911	0.943
IV	0.900	0.009	0.882	0.919
AHP	0.898	0.009	0.879	0.917

6. Conclusion

The most important facilitating factor in rock fall occurrence is slope angle, the highest weights of IV and AHP methods are gained for this factor and it is the most relevant factor in LR analysis. Earthquake intensity and geology are the next important factors.

IV and AHP weights for different classes of factors have rational trend based on pre-knowledge of rock fall occurrence, except for Slope Aspect, which is related neither to weathering parameters nor to earthquake waves' collision direction angle to the slope. Based on sensitivity analysis, the accuracy of the model results will reduce in absence of Slope Aspect; therefore, this parameter was preserved in the models.

The areas under the ROC curves are 0.927, 0.900, and 0.898 for LR, IV, and AHP methods respectively. LR seems to be the most suitable method for landslide hazard zonation of the study area, while all three methods have approximately similar qualities.

The area covered by Low and Very low hazard classes for three methods of LR, IV, and AHP are 76, 79, and 79 percent, respectively. The area of Low hazard class is overestimated in LR method relative

to other two methods. The area covered by High and Very high hazard classes for three methods of LR, IV, and AHP are 10, 12, and 12 percent, respectively. LR methods include the lowest Very High class area with the most density of rock fall.

References

1. Wilson, R.C. and Keefer, D.K. (1985) *'Predicting Areal Limits of Earthquake-Induced Landsliding'*. In: Earthquake Hazard in the Los Angeles Region, United States Government Printing Office, Washington, 317-346.
2. IRSC (2012) *Bulletin of Earthquakes*. Iran Seismological Center(IRSC). http://irsc.ut.ac.ir/bulletin.php.
3. Yaghmaei-Sabegh, S. (2014) Characteristics of near-Source ground motions from the 2012 Varzaghan-Ahar double earthquakes, northwest of Iran. *Nat Hazards*, **70**, 1077-1097.
4. LMO (2012) *Official Report of Legal Medicine Organization of Azerbaijan-E-Sharghi for Varzeghan-Ahar Earthquake*.
5. Memarian, P. and Mahdavifar, M. (2012) Distribution and characteristics of landslides induced by the Varzeghan Ahar earthquake doublet (Mw= 6.4 and Mw= 6.3) in 2012 in Azerbaijan-e-Sharghi, northwest of Iran. *Proceedings of the IPL Symposium*, 35-42.
6. Budimir, M., Atkinson, P., and Lewis, H. (2015) A Systematic review of landslide probability mapping using logistic regression. *Landslides*, 1-18.
7. Regmi, N.R., Giardino, J.R., McDonald, E.V., and Vitek, J.D. (2014) A comparison of logistic regression-based models of susceptibility to landslides in western Colorado, USA. *Landslides*, **11**(2), 247-262.
8. Marzorati, S., Luzi, L., and De Amicis, M. (2002) Rock falls induced by earthquakes: A statistical approach. *Soil Dynamics and Earthquake Engineering*, **22**(7), 565-577.
9. Keefer, D.K. (1984) Landslides caused by earthquakes. Geological Society of America Bulletin, **95**(4), 406-421.
10. Guzzetti, F., Carrara, A., Cardinali, M., and Reichenbach, P. (1999) Landslide hazard evaluation: A review of current techniques and their application in a multi-scale study, central Italy. *Geomorphology*, **31**(1), 181-216.
11. Glade, T. and Crozier, M.J. (2005) *'A Review of Scale Dependency in Landslide Hazard and Risk Analysis'*. In: Landslide Hazard and Risk, Wiley, Chichester, 75-138.
12. Kayastha, P., Dhital, M., and De Smedt, F. (2013) Application of the analytical hierarchy process (AHP) for landslide susceptibility mapping: A case study from the Tinau Watershed, west Nepal. *Computers & Geosciences*, **52**, 398-408.
13. Saadatkhah, N., Kassim, A., and Lee, L.M. (2014) Qualitative and quantitative landslide susceptibility assessments in Hulu Kelang area, Malaysia. *EJGE*, 19.
14. Murillo-Garcia, F.G. and Alcantara-Ayala, I. (2015) 'Landslide Susceptibility Analysis and Mapping Using Statistical Multivariate Techniques: Pahuatlan, Puebla, Mexico'. In: *Recent Advances in Modeling Landslides and Debris Flows*, Springer, 179-194.
15. Aleotti, P. and Chowdhury, R. (1999) Landslide hazard assessment: summary review and new perspectives. *Bulletin of Engineering Geology and the Environment*, **58**(1), 21-44.
16. Carrara, A., Cardinali, M., Guzzetti, F., and Reichenbach, P. (1995) 'GIS Technology in Mapping Landslide Hazard'. In: *Geographical nformation Systems in Assessing Natural Hazards*,Springer, 135-175.
17. Barredo, J., Benavides, A., Hervas, J., and Van Westen, C.J. (2000) Comparing heuristic landslide hazard assessment techniques using GIS in the Tirajana basin, Gran Canaria island, Spain. *International Journal of Applied Earth Observation and Geoinformation*, **2**(1), 9-23.
18. Nourani, V., Pradhan, B., Ghaffari, H., and Sharifi, S.S. (2014) Landslide susceptibility mapping at Zonouz plain, Iran using genetic programming and comparison with frequency ratio, logistic regression, and artificial neural network models. Natural Hazards, **71**(1), 523-547.

19. Zare, M., Kalantari, A., Ansari, A., Haghshenas, E., Davoodi, M., and Mostafazadeh, M. (2012) *Preliminary Report of Varzeghan-Ahar Earthquake Doublet*, 11 August 2012.

20. Vernant, P., Nilforoushan, F., Hatzfeld, D., Abassi, M., Vigny, C., Masson, F., Nankali, H., Martinod, J., Ashtiani, A., Bayer, R., Tavakoli, F., and Chery, J. (2004) Contemporary crustal deformation and plate kinematics in middle east constrained by GPS measurements in Iran and northern Oman. *Geophys. J. Int.*, 157, 381-398.

21. Copley, A., Faridi, M., Ghorashi, M., Hollingsworth, J., Jackson, J., Nazari, H., Oveisi, B., and Talebian, M. (2013) The 2012 August 11 Ahar earthquakes: Consequences for tectonics and earthquake hazard in the Turkish-Iranian plateau. *Geophysical Journal International*, **196**(1), 15-21.

22. Djamour, Y., Vernant, P., Nankali, H.R., and Tavakoli, F. (2011) NW Iran-Eastern Turkey present-day kinematics: results from the Iranian permanent GPS network. *Earth and Planetary Science Letters*, **307**(1-2), 27-34.

23. Copley, A. and Jackson, J. (2006) Active tectonics of the Turkish-Iranian plateau. *Tectonics*, **25**(6).

24. Ambraseys, N. and Melville, C. (1982) *A History of Persian Earthquakes*. Cambridge University Press, New York.

25. Berberian, M. and Yeats, R.S. (1999) Patterns of historical earthquake rupture in the Iranian plateau. *Bull. Seismol. Soc. Am.*, **89**(1), 129-139.

26. IIEES (2012) *Iran Seismic Catalogue*. http://www.iiees.ac.ir/.

27. Talebi, M., Zare, M., Mahdizadeh, R., and Bali-lashak, A. (2015) Spatial-temporal analysis of seismicity before the 2012 Varzeghan, Iran, Mw 6.5 earthquake. *Turkish Journal of Earth Sciences*, **24**(3), 289-301.

28. Kassam, A.H. (1981) Climate, soil and land resources in north Africa and west Asia. *Plant and Soil*, 58, 1-28.

29. Delju, A.H., Ceylan, A., Piguet, E., and Rebetez, M. (2013) Observed climate variability and change in Urmia Lake basin, Iran. *Theoretical and Applied Climatology*, **111**(1), 285-296.

30. Kehl, M. (2009) Quaternary climate change in Iran - the state of knowledge. *Erdkunde - Archive for Scientific Geography*, **63**(1), 1-17.

31. IRMO (2012) *Iran Meteorological Organization (IRMO)*, Bureau of Meteorology east Azerbaijan statistics. http://www.eaz.ir/english/.

32. Amidi, M., Lescuyer, J.L., and Riou, R. (1978) Geologic Quadrangle Map of Ahar (1:250,000). *Geological Survey of Iran* (GSI), Tehran.

33. Manouchehri, M., Hosseini, Z., Afsharianzadeh, A., and Chaichi, Z. (1989) Geologic Quadrangle Map of Tabriz-Poldasht(1:250,000). *Geological Survey of Iran* (*GSI*), Tehran.

34. Rajabi, A.M., Khamehchiyan, M., Mahdavifar, M., Del Gaudio, V., and Capolongo, D. (2013) A time probabilistic approach to seismic landslide hazard estimates in Iran. *Soil Dynamics and Earthquake Engineering*, **48**, 25-34.

35. Baron, I., Kernstockova, M., Faridi, M., Bubik, M., Milovsky, R. Melichar, R. Sabouri, J., and Baburek, J. (2013) Paleostress analysis of a gigantic gravitational mass movement in active tectonic setting: The Qoshadagh slope failure, Ahar, NW Iran. *Tectonophysics*, **605**, 70-87.

36. Cornforth, D.H. (2005) *Landslides in Practice-Investigation, Analysis, and Remedial Preventative Options in Soils*. John Wiley & Sons Inc., New Jersey.

37. Süzen, M.L. and Kaya, B.S. (2012) Evaluation of environmental parameters in logistic regression models for landslide susceptibility mapping. *International Journal of Digital Earth*, **5**(4), 338-355.

38. Yin, K. and Yan, T. (1988) Statistical prediction model for slope instability of metamorphosed rocks. *Proceedings of the 5th International Symposium on Landslides*, *Lausanne, Switzerland*, **2**, 1269-1272.

39. Wu, S., Shi, L., Wang, R., Tan, C., Hu, D., Mei, Y., and Xu, R. (2001) Zonation of the landslide hazards in the forereservoir region of the Three

Gorges project on the Yangtze river. *Engineering Geology*, **59**(1), 51-58.

40. Kelarestaghi, A. and Ahmadi, H. (2009) Landslide susceptibility analysis with a bivariate approach and GIS in Northern Iran. *Arabian Journal of Geosciences*, **2**(1), 95-101.
41. Klose, M., Gruber, D., Damm, B., and Gerold, G. (2014) Spatial databases and GIS as tools for regional landslide susceptibility modeling. *Zeitschrift für Geomorphologie*, **58**(1), 1-36.
42. Akbar, T.A. and Ha, S.R. (2011) Landslide hazard zoning along Himalayan Kaghan valley of Pakistan by integration of GPS, GIS, and remote sensing technology. *Landslides*, **8**(4), 527-540.
43. Cox, D.R. (1958) The regression analysis of binary sequences. *Journal of the Royal Statistical Society*. Series B (Methodological), **20**(2), 215-242.
44. Johnson, D.E. (1998) *Applied Multivariate Methods for Data Analysts*. Duxbury Resource Center.
45. Chauhan, S., Sharma, M., and Arora, M.K. (2010) Landslide susceptibility zonation of the Chamoli region, Garhwal Himalayas, using logistic regression model. *Landslides*, **7**(4), 411-423.
46. Saaty, T.L. (1977) A scaling method for priorities in hierarchical structures. *Journal of Mathematical Psychology*, **15**(3), 234-281.
47. Saaty, T.L. (2008) Decision making with the analytic hierarchy process. *International Journal of Services Sciences*, **1**(1), 83-98.
48. Saaty, T.L. (1980) *The Analytic Hierarchy Process: Planning, Priority Setting, Resources Allocation*. McGraw-Hill, New York.
49. Saaty, T.L. and Vargas, L.G. (2012) *Models, Methods, Concepts & Applications of the Analytic Hierarchy Process*. Springer Science & Business Media.
50. Rezaie, F. and Panahi, M. (2015) GIS modeling of seismic vulnerability of residential fabrics considering geotechnical, structural, social and physical distance indicators in Tehran using multi-criteria decision-making techniques. *Natural Hazards and Earth System Science*, **15**(3), 461-474.
51. Ying, X., Zeng, G.M., Chen, G.Q., Tang, L., Wang, K.L., and Huang, D.Y. (2007) Combining AHP with GIS in synthetic evaluation of eco-environment quality-a case study of Hunan province, China. *Ecological Modelling*, **209**(2), 97-109.
52. Rodriguez, C., Bommer, J., and Chandler, R. (1999) Earthquake-induced landslides: 1980-1997. *Soil Dynamics and Earthquake Engineering*, **18**(5), 325-346.
53. Dai, F., Xu, C., Yao, X., Xu, L., Tu, X., and Gong, Q. (2011) Spatial distribution of landslides triggered by the 2008 Ms 8.0 Wenchuan earthquake, China. *Journal of Asian Earth Sciences*, **40**(4), 883-895.
54. Mahdavifar, M.R., Solaymani, S., and Jafari, M.K. (2006) Landslides triggered by the Avaj, Iran earthquake of June 22, 2002. *Engineering Geology*, **86**(2), 166-182.
55. Khazai, B. and Sitar, N. (2004) Evaluation of factors controlling earthquake-induced landslides caused by Chi-Chi earthquake and comparison with the Northridge and Loma Prieta events. *Engineering Geology*, **71**(1), 79-95.
56. Parker, R., Hancox, G., Petley, D., Massey, C., Densmore, A., and Rosser, N. (2015) Spatial distributions of earthquake-induced landslides and hillslope preconditioning in northwest South Island, New Zealand. *Earth Surface Dynamics Discussions*, **3**(4), 501-525.
57. Baeza, C. and Corominas, J. (2001) Assessment of shallow landslide susceptibility by means of multivariate statistical techniques. *Earth Surface Processes and Landforms*, **26**(12), 1251-1263.
58. Hanley, J.A. and McNeil, B.J. (1983) A method of comparing the areas under receiver operating characteristic curves derived from the same cases. *Radiology*, **148**(3), 839-843.
59. Mathew, J., Jha, V., and Rawat, G. (2009) Landslide susceptibility zonation mapping and its validation in part of Garhwal Lesser Himalaya, India, using binary logistic regression analysis and receiver operating characteristic curve method. *Landslides*, **6**(1), 17-26.